



ARTICLE

Robotic integration enables autonomous operation of laboratory scale stirred tank bioreactors with model-driven process analysis

Holger Morschett¹ | Niklas Tenhaef¹ | Johannes Hemmerich¹ | Laura Herbst¹ | Markus Spiertz¹ | Deniz Dogan¹ | Wolfgang Wiechert^{1,2} | Stephan Noack¹  | Marco Oldiges^{1,3} 

¹Institute of Bio- and Geosciences, IBG-1: Biotechnology, Forschungszentrum Jülich GmbH, Jülich, Germany

²Computational Systems Biotechnology, RWTH Aachen University, Aachen, Germany

³Institute of Biotechnology, RWTH Aachen University, Aachen, Germany

Correspondence

Marco Oldiges, Institute of Bio- and Geosciences, IBG-1: Biotechnology, Forschungszentrum Jülich GmbH, Wilhelm-Johnen-Straße, 52428, Jülich, Germany.
Email: m.oldiges@fz-juelich.de

Funding information

Bundesministerium für Bildung und Forschung, Grant/Award Numbers: 031B0463, 031B0918A; Helmholtz-Gemeinschaft, Grant/Award Number: "Helmholtz Innovation Labs" program

Abstract

Given its geometric similarity to large-scale production plants and the excellent possibilities for precise process control and monitoring, the classic stirred tank bioreactor (STR) still represents the gold standard for bioprocess development at a laboratory scale. However, compared to microbioreactor technologies, bioreactors often suffer from a low degree of process automation and deriving key performance indicators (KPIs) such as specific rates or yields often requires manual sampling and sample processing. A widely used parallelized STR setup was automated by connecting it to a liquid handling system and controlling it with a custom-made process control system. This allowed for the setup of a flexible modular platform enabling autonomous operation of the bioreactors without any operator present. Multiple unit operations like automated inoculation, sampling, sample processing and analysis, and decision making, for example for automated induction of protein production were implemented to achieve such functionality. The data gained during application studies was used for fitting of bioprocess models to derive relevant KPIs being in good agreement with literature. By combining the capabilities of STRs with the flexibility of liquid handling systems, this platform technology can be applied to a multitude of different bioprocess development pipelines at laboratory scale.

KEYWORDS

laboratory automation, maximum likelihood estimation, process control system, robotic integration, stirred tank bioreactor

Abbreviations: API, application programming interface; CDW, cell dry weight (g L^{-1}); CV, coefficient of variation (%); GFP, green fluorescent protein; IPTG, isopropyl- β -D-thiogalactopyranoside; KPI, key performance indicator; MTP, microtiter plate; OD, optical density; ODE, ordinary differential equation; PCS, process control system; q_s , biomass-specific substrate uptake rate [$\text{g g}^{-1} \text{h}^{-1}$]; STR, stirred tank bioreactor; $Y_{P/X}$, biomass-specific product yield [g g^{-1}]; $Y_{X/S}$, substrate-specific biomass yield [g g^{-1}]; μ_{max} , maximum growth rate [h^{-1}].

Holger Morschett, Niklas Tenhaef, and Johannes Hemmerich contributed equally to this study.

This is an open access article under the terms of the [Creative Commons Attribution License](https://creativecommons.org/licenses/by/4.0/), which permits use, distribution and reproduction in any medium, provided the original work is properly cited.

© 2021 The Authors. *Biotechnology and Bioengineering* published by Wiley Periodicals LLC

1 | INTRODUCTION

Bioprocess development faces the challenge of investigating a large set of interconnected parameters and adjusting them to optimal values in the least amount of time possible. In the interests of cost, time and resource efficiency, new processes are firstly developed at laboratory scale (Doig et al., 2006; Marques et al., 2010). Once specified key performance indicators (KPIs) have been reached, the processes are gradually scaled up to the production environment. Given its geometric similarity to large-scale production plants and the excellent possibilities for precise process control and monitoring, the classic stirred tank bioreactor (STR) is considered the gold standard for bioprocess development at a laboratory scale.

Among the key parameters of every bioprocess are concentrations of biomass, substrate, and product, laying the basis to derive KPIs, such as yields or specific rates as intrinsic properties of the investigated microbial process. Today, various on-line and in-line probes are available for process analytics, often based on the use of optical or spectroscopic methods. Selected examples can be found in studies by Tamburini et al. (2014), Kreyenschulte et al. (2015), and Lee et al. (2004). However, these technologies typically suffer from specific drawbacks like limited measuring ranges, interference by dispersed gas, (bio-)fouling or the necessity of using advanced models and extensive calibration (Chmiel, 2011; Vojinović et al., 2006). In addition, automated methods for sample-based analysis, for example via at-line high performance liquid chromatography (Tohmola et al., 2011) or flow injection coupled to biosensors (Peuker et al., 2004), are available. A common aspect of the above-mentioned methods is the typically high effort for setup and maintenance, so that their application with STRs in research environments with frequently changing microbial systems and bioprocess conditions may be difficult to justify.

Thus, relevant measures are often acquired manually using sampling-based off-line methods. Although autosamplers can be used as a support, they only handle the actual sampling, but not the subsequent processing and analysis. Consequently, manual operation of STRs necessitates extensive hands-on-time if data is acquired with appropriate temporal resolution and conflicts with regulated working hours arise easily. Additional effort is needed if dynamic adjustments and decision making is required based on monitoring certain variables at runtime followed by event-based triggering. For example, in the case of inducible expression of heterologous protein, where premature induction may easily lead to reduced overall performance (Huber et al., 2009). Here, high temporal resolution of biomass concentration is crucial for optimal timing of induction events.

Coupled with the increasing propagation of advanced microcultivation systems (Hemmerich, Noack, et al., 2018), a variety of technologies for laboratory automation have found their way into research and development laboratories over the past two decades (Baumann et al., 2015; Cruz Bournazou et al., 2017; Funke et al., 2010; Hemmerich, Tenhaef, et al., 2018; Heux et al., 2014; Puskeiler et al., 2005; Rohe et al., 2012). By integrating liquid

handling robots and other connected devices such as centrifuges, microtiter plate (MTP) readers and others, automated microcultivation platforms have been created that fundamentally changed the way process developers work. Nowadays, microscale cultivation processes allow parallelized approaches to a high extent but can also be automated to a large degree. This includes preparatory work, as well as sampling and sample processing up to analysis.

The application of such automation strategies must not be limited to microbioreactor systems, and thus, there are strong arguments that suggest generalizing automation technologies towards a modularized solution for automated operation for laboratory scale STR processes. In this study, such platform was realized by coupling four parallelized STRs to a liquid handling robot. A custom-made process control system (PCS) based on Python was developed, integrating a higher-level process intelligence to orchestrate different monitoring and control modules: (1) automated inoculation, (2) biomass-triggered induction, (3) discontinuous sampling with at-line quantification of biomass, product, and substrate as well as (4) model-driven estimation of KPIs for in-depth process analysis.

2 | MATERIALS AND METHODS

2.1 | Chemicals, strain, and media

All chemicals were obtained from Sigma-Aldrich or Roth and were of analytical grade. *Corynebacterium glutamicum* ATCC13032 was used for all cultivation experiments. The strain carried a pEKEx2 plasmid for isopropyl- β -D-1-thiogalactopyranoside (IPTG)-inducible expression of a pCGPhoD^{Cg}-GFP fusion protein being secreted via the twin-arginine translocation pathway (Meissner et al., 2007) and was cultivated in CGXII medium (Keilhauer et al., 1993): 41.85 g 3-(N-morpholino)propanesulfonic acid (shake flask only), 20 g glucose (varied during STR experiments), 20 g (NH₄)₂SO₄, 5 g (NH₂)₂CO (shake flask only), 1 g KH₂PO₄, 1 g K₂HPO₄, 1 g MgSO₄·7H₂O, 13.25 mg CaCl₂·2H₂O, 50 mg kanamycin sulfate, 30 mg protocatechuic acid, 10 mg FeSO₄·7H₂O, 10 mg MnSO₄·H₂O, 1 mg ZnSO₄·7H₂O, 0.313 mg CuSO₄·5H₂O, 0.2 mg biotin, 0.02 mg NiCl₂·6H₂O (all values refer to 1 L of cultivation medium). The pH was adjusted to 7 using 4 M NaOH and 0.2% (v⁻¹) antifoam 204 (Sigma-Aldrich) was added for STR cultivation.

2.2 | Cultivation

2.2.1 | Strain maintenance

Exponentially growing cells from STR cultivation were harvested, centrifuged for 5 min at 9283g in a GS-15 R (Beckman Coulter), resuspended to an optical density (OD) of 40 in 50% (w v⁻¹) glycerol with 0.9% (w v⁻¹) NaCl and 1 ml aliquots were frozen to -80°C for storage.

2.2.2 | Precultivation

Fifty milliliter medium was inoculated with 150 μL cryoculture and incubated in a fourfold baffled 500 mL shake flask at 30°C, 300 rpm and 25 mm shaking diameter in a Multitron Pro incubator (Infors). The culture was harvested during exponential growth as monitored by an SFR Vario (PreSens), centrifuged for 5 min at 9283g in a GS-15R and resuspended in approx. 20 mL 0.9% (w v⁻¹) NaCl to obtain a stock suspension for the inoculation of STRs.

2.2.3 | STR cultivation

Cultures were run in a fourfold parallelized glass STR setup equipped with two Rushton impellers each (Dasgip) at 30°C and gassing with compressed air was maintained at 60 NL_{gas}•L_{liquid}⁻¹•h⁻¹. Starting volume was 1 L (batch) or 0.8 L (fed-batch). pH was monitored with 405-DPAS-SC-K8S/225/120 electrodes (Mettler Toledo) and titrated to 7 using 25% (w v⁻¹) NH₃ (aq) and 7 M H₃PO₄. Dissolved oxygen was measured by VisiFerm DO 225 optodes (Hamilton) and regulated to $\geq 30\%$ using a stirrer cascade (400–1400 rpm).

2.3 | Automated at-line procedures

Automated at-line procedures were performed on a Freedom EVO 200 robotic platform equipped with a liquid handling arm with eight steel tips and a robotic manipulator (Tecan). An Infinite M 200 Pro MTP reader (Tecan), a Rotanta 460 RSC MTP centrifuge (Hettich) as well as a custom-made station for stirring of suspensions in 50 mL beakers based on a MIXdrive 1 XS magnetic stirrer controlled by a MIXcontrol 20 unit (2mag) were additionally integrated. One of the MTP carriers on the robotic worktable was coupled to a Microcool MC 600 refrigerated circulator (Lauda). The whole robotic platform was equipped with a laminar flow hood with HEPA filters ensuring a sterile environment above the robotic worktable. The worktable itself was thoroughly cleaned with ethanol before each experiment.

A setup for robotic dead-end dosing and sampling was developed. Instead of a riser pipe, each STR was equipped with a custom-made glass port below liquid level being designed not to induce dead zones to the bulk liquid while simultaneously having only minimal inner volume (Figure 1a). Via Bioprene tubes (1.0 mm inner diameter, Watson-Marlow) the ports were connected to an automation module (Figure 1b) placed on the robotic worktable in reach of the liquid handling arm. For each of the four channels, it carried a pierceable silicone septum as sterile barrier. The whole setup is fully autoclavable ensuring straightforward operability. The total inner volume was $\sim 350 \mu\text{L}$ per channel.

2.3.1 | Sampling

Upon each sampling event triggered by the PCS 950 μL sample was withdrawn from each individual STR via the respective channel applying the following steps: (1) covering of septum with ethanol, (2) sampling and discarding of 950 μL to exchange inner volume of the channel, (3) sampling 950 μL , (4) removing and discarding of ethanol above the septum. Depending on gas hold-up, varying fractions of dispersed gas may be co-aspirated during sampling, resulting in reduced accuracy. Moreover, small gas bubbles may remain within the sampled liquid and can interfere with optical biomass measurement. Therefore, bubbles were removed by slow dispense into a 96-deepwell MTP (Ritter) and re-aspiration of the needed volume for subsequent steps. Additionally, pipetting parameters were optimized towards removing dispersed gas from the liquid.

2.3.2 | Biomass quantification

At-line biomass was acquired as absorption at 600 nm in the MTP photometer using 250 μL cell suspension in 96-well MTPs (Greiner Bio-One). If needed, samples were diluted in 200 mM 3-(N-morpholino)propanesulfonic acid (pH 7) while decision on the appropriate dilution factor was made by the PCS (Section 2.5).

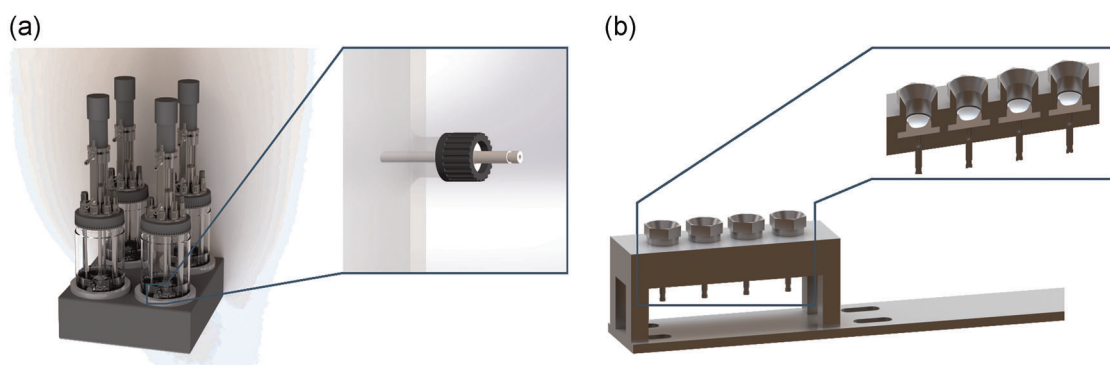


FIGURE 1 Hardware setup. (a) Four parallelized laboratory scale STRs are equipped with a low-volume port below the liquid level. (b) The ports are connected to a custom-built automation module allowing for sterile dosing and sampling operations using a liquid handling robot. STR, stirred tank bioreactor [Color figure can be viewed at wileyonlinelibrary.com]

2.3.3 | Cell separation

After biomass measurement (Section 2.3.2), cells in the remaining sample were separated by 5 min centrifugation at 2400g in the robotic centrifuge and cell-free supernatants were used for further analysis.

2.3.4 | Glucose quantification

Glucose was quantified using a hexokinase assay (DiaSys) in 96-well MTP format. Using the robotic platform, cell-free supernatants (Section 2.3.3) were appropriately diluted in 0.9% (w v⁻¹) NaCl, 20 μ L were mixed with 280 μ L assay mastermix and incubated for 6 min at room temperature before absorption measurement at 365 nm in the MTP reader. Results were calibrated against glucose standards (0.025–2 gL⁻¹) processed in the same way.

2.3.5 | Protein quantification

Green fluorescent protein (GFP) was measured in 250 μ L cell-free supernatant obtained from robotic cell separation (Section 2.3.3). Fluorescence at 520 nm was acquired after excitation at 488 nm in the MTP reader using 96-well MTPs while decision on the appropriate dilution factor was made by the PCS (Section 2.5).

2.3.6 | Inoculation

Inoculation stock suspension (Section 2.2.1) was placed in the stirring station in a pre-sterilized 50 mL beaker and mixed at 400 rpm. Using 0.9% (w v⁻¹) NaCl a dilution series of the suspension was automatically prepared and absorption was measured in the MTP reader (Section 2.3.2) in technical replicates ($n = 8$). Stirring was paused during aspiration to maintain pipetting accuracy. Based on the target inoculation density initially defined by the operator, the needed volume was calculated and injected into the STRs. In contrast to sampling (Section 2.3.1), exchange of the inner volume of the respective channels was skipped. Instead, 950 μ L sterile water was injected directly after dosing the inoculum to ensure the latter was completely transferred into the STR bulk volume.

2.3.7 | Induction

Biomass concentration exceeding a threshold previously defined by the operator triggered automated induction upon which 250 μ L IPTG stock (1 M) was injected into the respective STR via the automation module applying the dosing procedure as used for inoculation (Section 2.3.6). Before usage, IPTG stocks were maintained at 4°C in a custom-build aluminum MTP sealed with a pierceable sterile foil placed on the cooling carrier on the robotic worktable.

2.4 | Off-line determination of biomass, glucose, and protein

OD (600 nm) was measured in 10 mm polystyrene semi-micro cuvettes (ratiolab) using an UV-1800 photometer (Shimadzu). Samples were diluted in 0.9% (w v⁻¹) NaCl to fit the linear range if necessary.

For cell dry weight (CDW) measurement, 1.5 mL cell suspension was centrifuged at 16,060g for 10 min in a dried and pre-weighed reaction tube in a Biofuge Pico (Heraeus) and the supernatant was removed. The pellet was dried at 80°C for 24 h, acclimated in a desiccator and weighed. CDW was calculated from the mass difference.

Off-line glucose quantification was done with the same procedure as reported in Section 2.3.4.

Extracellular protein was measured using the Pierce BCA Protein Assay Kit (Thermo Fisher Scientific) in 96-well MTP format according to manufacturer's specifications. Samples were diluted in 0.9% (w v⁻¹) NaCl whenever necessary. As an alternative, off-line GFP fluorescence measurements were conducted as described in Section 2.3.5.

2.5 | Python-based PCS

An object-oriented Python-based PCS was developed to orchestrate the actions of the liquid handling robotic platform according to the needs of the experiment (Figure 2). It consists of the "auto_str" module and several submodules. The "auto_str" module is imported by a Python script referred to as "experiment.py", which defines the basic order of operations and loads the settings file to be used. Settings files are in yaml format (Ben-Kiki et al., 2009) and hold essential information like sampling times, induction trigger values, pipetting volumes, file paths, and more. Every experiment involves three stages: preparation, sampling loop, and finalization. The sampling loop runs for as many cycles as there were sampling times defined in the settings. In each cycle, robotic actions are triggered, data is parsed, analyzed, and stored and decisions, for example, about dilutions for the subsequent cycle, are made.

While all glucose measurements were conducted at the same dilution, for biomass and GFP a series of dilution levels was defined, resulting in a series of nested measurement ranges. Dilutions were performed in a single- or two-step workflow focusing on minimal pipetting errors dependent on the actual volumes to be transferred. Initial measurements were done with the lowest dilution feasible. In case the actual measurement exceeded the center point of the current measurement range, the dilution was incremented to its respective next level in the subsequent cycle. Nesting of the individual classes has been designed in such a way that a suitable measurement range is always provided when changing classes and no gaps can occur. This even applies if the measured value has significantly decreased in the corresponding cycle against all expectations. This ensured a fully autonomous selection of the suitable dilution stage (Figure S1).

The experiment logic itself is defined in the "Experiment" class within the "auto_str" module. Instantiation of this class also creates the necessary data structures utilizing pandas (McKinney, 2010) and NumPy (Harris et al., 2020; van der Walt et al., 2011). The class

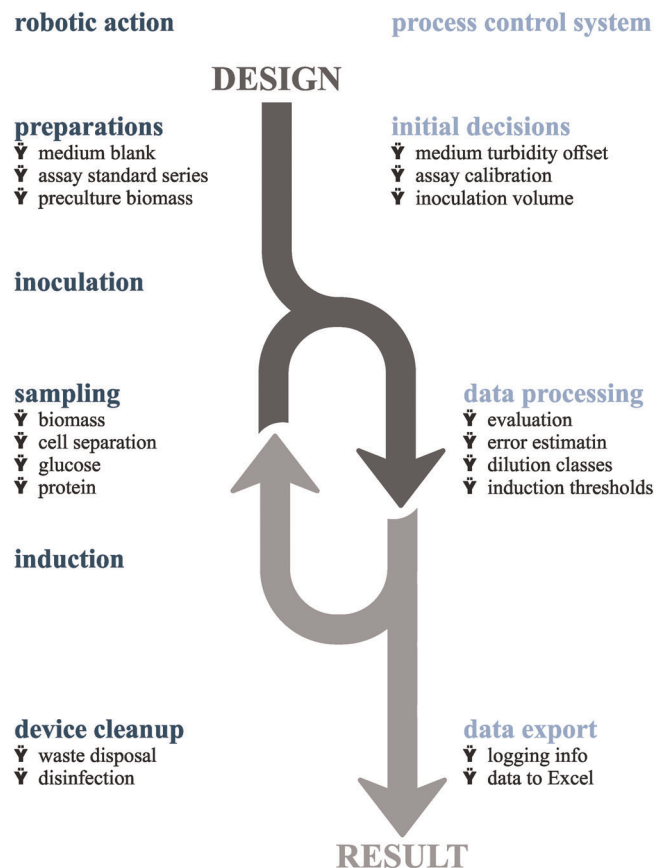


FIGURE 2 Schematic representation of experimental workflow with individual tasks being orchestrated by the Python-based PCS. PCS, process control system [Color figure can be viewed at [wileyonlinelibrary.com](https://onlinelibrary.wiley.com)]

utilizes submodules, for example, for execution of liquid handling actions and for parsing of data files from the utilized MTP reader.

Control of the liquid handling platform is realized by the provided application programming interface (API) via pythonnet (Cline et al., 2019). Its basic function is to trigger predefined robotic scripts, representing individual workflow steps. While this is sufficient in most cases, a notable exception is the script which triggers measurement processes of the MTP reader: Here, it was necessary to change the wells and MTPs to be measured alongside the sampling cycles which is not possible via the API. A customized solution was realized by saving the respective robotic script as a template with placeholders for the dynamic parts (i.e., well numbers and plate positions on the robotic worktable). During the experiment run, the template was loaded, the placeholders were substituted depending on the individual cycle, the script was saved, and its execution triggered by the API. After liquid handling actions and MTP reader measurements, data from the MTP reader was parsed using pandas and analyzed using SciPy (Virtanen et al., 2020).

2.6 | Estimation of bioprocess model parameters

A model-based approach was chosen to derive KPIs from cultivation data stemming from different bioprocess designs. To describe the

nonlinear dynamics in concentrations of biomass, substrate, and product, classical bioprocess modelling based on systems of ordinary differential equations (ODEs) was performed.

In this study, some model parameters (yield coefficients) and metrics derived thereof (prediction of maximum product titer) were defined as KPIs of interest (cf. application studies). Model parameters were estimated based on all data from the independent parallel cultivations using the “pyFOOMB” package (Hemmerich, Tenhaef, et al., 2021). This package allows an object-oriented implementation of ODE-based models and provides convenient routine methods, for example, fitting models to experimental data. Having full programmatic access via the Python language, seamless integration with other packages for scientific computing in highly customized workflows is facilitated, for example, with the PCS developed in this study.

For parameter estimation including uncertainty analysis, parallelized parametric bootstrapping was applied (see Hemmerich, Tenhaef, et al. (2021) for more details). From the obtained distributions parameter values and lower/upper uncertainty bounds were derived as medians and 2.5%–97.5% percentiles, respectively. A detailed description of applied ODE models is provided in Supporting Information Section 1.

3 | RESULTS AND DISCUSSION

3.1 | Automated at-line measurements

Time series of biomass, substrate, and product as well as corresponding KPIs are essentially valuable for the in-depth description of bioprocesses. In the present study suitable technology and methods were developed, such as customized sampling ports for laboratory scale STRs, a hardware interface to the robotic system as well as a modular PCS. Special focus was put on the consistent application of optical measurement techniques since these provide results comparatively quickly without specialized analytical instrumentation except for an MTP reader and are therefore predestined for at-line process monitoring. The biomass measurement technique by optical density and the applied assays for substrate and product quantification provide a universal framework for fast at-line analytics. The applied methods for substrate and product quantification can be considered as prototypic blueprints for a broad range of possible future applications. In terms of a modular architecture, they can be easily exchanged for other procedures to meet the specific requirements of the bioprocess under investigation.

3.1.1 | At-line biomass

In analogy to well-established off-line measurement of biomass by OD (Sonnleitner et al., 1992), absorption at 600 nm was acquired from crude cell suspension samples in MTPs. Here, 250 μ L volume per well proved optimal with respect to reproducibility as revealed in

preliminary experiments (Figure S2). As shown in Figure 3a, precisely acquired at-line OD (1.4% average coefficient of variation (CV) for $n \geq 3$ technical replicates) could be correlated with CDW measurement by a second order polynomial within 0.05–0.80 g L⁻¹ CDW. Thereby, already low biomass levels typically occurring at the beginning of bioprocesses can be tracked. Higher biomass concentration can be measured by appropriate sample dilution to meet the calibrated range of the method. Therefore, decision logics for appropriate sample dilution were necessary and implemented into the PCS as described in detail in Section 2.5.

3.1.2 | At-line glucose

At-line quantification of glucose implicates short data acquisition times as well as a high dynamic range to keep the needed number of dilution steps as low as possible. To meet these demands an enzymatic assay converting glucose to gluconate-6-phosphate was used. Equimolar amounts of NADH formed are measured by 365 nm absorption.

Characterization with standards revealed a linear range from 0.025 to 2 g L⁻¹ (Figure 3b). Due to this wide dynamic range, all cultivation samples could be handled with a single dilution level defined by the glucose concentration applied during the respective cultivation. Thereby, the full range of expected concentrations could be covered at minimal number of analyses. For the given range stable endpoint absorption was always achieved within 6 min (Figure 3c) enabling fast data acquisition with less than 8 min from supernatants to available concentration results.

During automated cultivation processes, all measurements were performed from the same assay mastermix stored on the robotic worktable and constant performance for at least 140 h was confirmed for storage at room temperature (Figure S3). Thus, one single calibration acquired during the preparation phase could be used, rather than repeated calibrations for individual sampling events.

Microbial cultivation is often coupled to formation of various by-products like organic acids (Paczia et al., 2012) and such compounds may disturb analytics either by side reactions or by changing reactivity of the applied enzyme system (Bisswanger, 2014; Passonneau & Lowry, 1993). Selected compounds from microbial

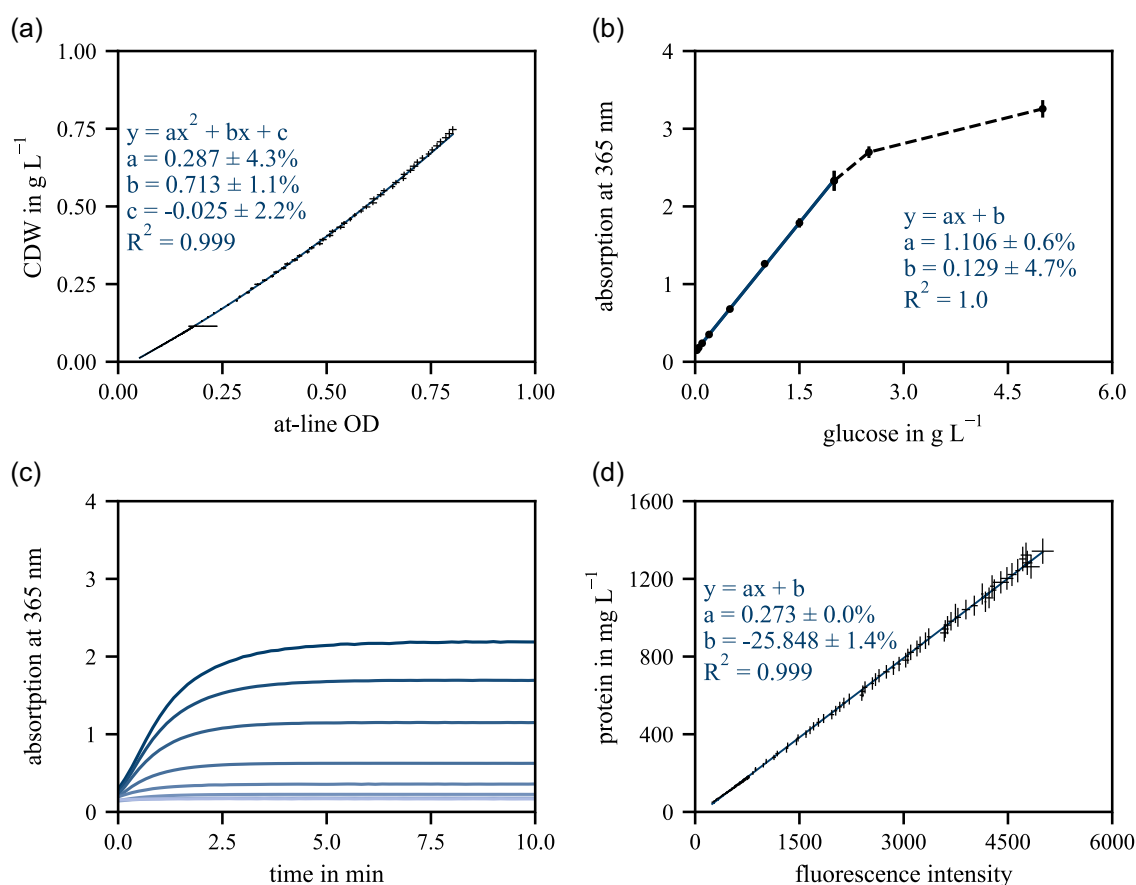


FIGURE 3 Evaluation of at-line procedures. (a) Calibration of CDW (gravimetric method) against at-line acquired OD (MTP reader). Optical measures at 600 nm and 250 μ L liquid volume. Error bars derived from technical replicates ($n \geq 3$). (b) Linear range of the assay. Error bars derived from technical replicates ($n = 5$). (c) Reaction progress at different initial glucose concentrations (0.025–2 g L⁻¹, indicated by gradually decreasing color transparency). (d) Calibration of extracellular protein concentration (bicinchoninic acid assay) against respective at-line GFP fluorescence (MTP reader). Error bars derived from technical replicates ($n = 5$). CDW, cell dry weight; GFP, green fluorescent protein; MTP, microtiter plate [Color figure can be viewed at wileyonlinelibrary.com]

central and overflow metabolism (e.g., lactate, malate, succinate) were checked for interfering effects while none of the tested species had an effect when 25 mM were spiked into glucose standards (Figure S4). Consequently, up to 250 mM of tested agents may be present in samples in case of 10-fold dilution without effect on glucose quantification which is far beyond expected concentrations for the given model system.

3.1.3 | At-line protein

In analogy to biomass (Section 3.1.1), secreted protein was also monitored optically. GFP-specific fluorescence at 520 nm could be precisely measured in MTPs (1.4% average CV from $n = 5$ technical replicates) after excitation at 488 nm (Section 2.3.5) of cell-free supernatants (Section 2.3.3). Translation of fluorescence by external calibration using a bicinchoninic acid assay (Section 2.4) enabled at-line quantification of secreted protein in a range of 50–1340 mg L⁻¹ protein by linear regression (Figure 3d). In analogy to biomass measurements decision logics for appropriate at-line dilution were implemented into the PCS (Section 2.5).

3.2 | Proof of concept: Variation of glucose concentration

Following hardware implementation (Section 2.3) and the establishment of the robotic workflows, all procedures were embedded into the PCS (Section 2.5) and the full setup was tested during a proof-of-concept study where GFP-secreting *C. glutamicum* was cultivated in batch mode at three different initial glucose concentrations. All cultures were induced with IPTG from the start. The following tasks were addressed at-line by the automated workflows and hardware system: (1) inoculation to 0.05 g L⁻¹ CDW from a pre-culture provided on the robotic worktable, (2) sampling of all reactors at 60 min interval, (3) measurement of biomass concentration with choice of appropriate dilution level, (4) cell separation, (5) measurement of extracellular glucose (fixed sample dilution sufficient) and protein concentration from cell-free supernatants.

As shown in Figure 4, biomass formation could successfully be tracked via calibrated absorption measurements in all three STRs at 3.1% average CV. Corresponding glucose consumption was monitored via the enzymatic assay at 5.7% average CV. Also, the course of secreted GFP was tracked by fluorescence measurements at 4.4% average CV. Thus, along 24 samples a total of 72 measurements were taken per reactor, all fully automated without any interference by the operator and thereby without gaps due to nighttime.

Data was fitted to an ODE model based on Monod kinetics and growth-coupled protein production (Supporting Information Section 1.1). It can be seen that the model adequately describes the experimental time series (Figure 4) and only minor deviations in the biomass concentrations are visible after glucose depletion. Table 1 provides an overview for selected KPIs.

Estimates for maximum growth rate μ_{\max} , biomass-specific substrate uptake rate $q_{S\max}$, and substrate-specific biomass yield coefficient $Y_{X/S}$ are in good agreement with literature data for the corresponding wild type (Grünberger et al., 2013; Hemmerich, Tenhaef, et al., 2018; Rohe et al., 2012; Unthan et al., 2014). Although there is no literature known to the authors reporting on $Y_{P/X}$, estimates are within reasonable range.

Overall, the proof-of-concept study showed that the developed workflow is suitable for automated operation of parallelized

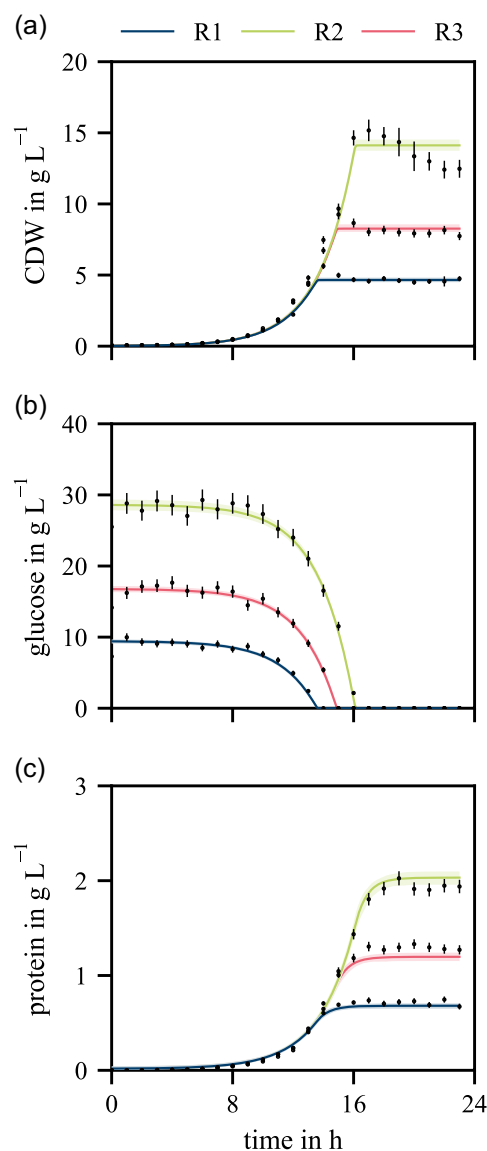


FIGURE 4 Proof-of-concept cultivation experiment for autonomous STR operation workflow with three individual reactors at different initial glucose concentrations. (a) Biomass. (b) Glucose. (c) Extracellular protein. Dots represent measured data with error bars representing measurement error estimated by parametric bootstrapping ($n = 10,000$). Lines represent medians from 250 corresponding model fits with shaded areas as 2.5%–97.5% percentiles (Section 2.6). STR, stirred tank bioreactor [Color figure can be viewed at wileyonlinelibrary.com]

	μ_{\max} (h^{-1})	q_{Smax} ($\text{g}\cdot\text{g}^{-1}\cdot\text{h}^{-1}$)	q_{Pmax} ($\text{g}\cdot\text{g}^{-1}\cdot\text{h}^{-1}$)	$Y_{\text{X/S}}$ (g g^{-1})	$Y_{\text{P/X}}$ (g g^{-1})
Median	0.43	0.86	0.061	0.49	0.14
2.5%–97.5% percentile	0.40–0.45	0.82–0.90	0.057–0.064	0.47–0.51	0.13–0.15

TABLE 1 Fitting results and derived KPIs of the proof-of-concept cultivation

Note: Median values and uncertainties derived from 250 model fits per cultivation set (Section 2.6).

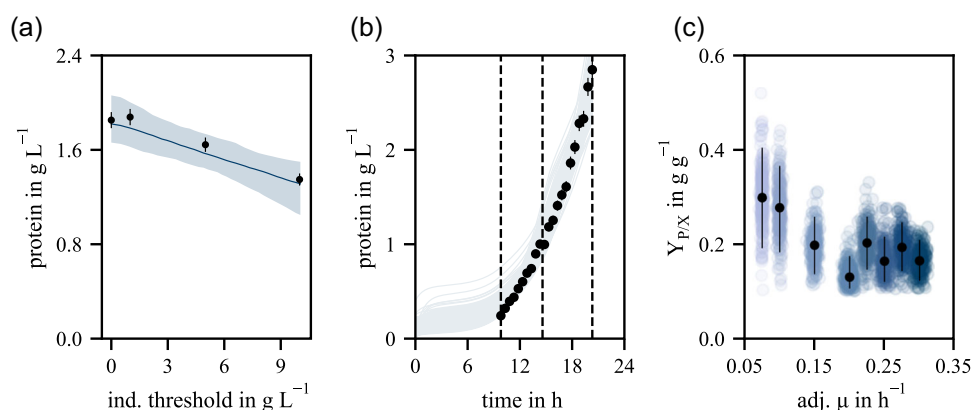


FIGURE 5 Application studies. (a) Induction profiling: Individual reactors were induced by IPTG dosage when crossing predefined CDW thresholds. Dots represent measured data with error bars representing measurement error estimated by parametric bootstrapping ($n = 10,000$). Line represents median from 250 corresponding model fits with shaded areas as 2.5%–97.5% percentiles. (b) Exemplary representation of protein concentration time series of a single STR during exponential feeding at two different rates. Dots represent measured data with error bars derived from accuracy of underlying unit operations by parametric bootstrapping ($n = 10,000$). Blue lines represent outcome of 250 corresponding model fits. (c) Biomass-specific product yield for eight different adjusted exponential growth rates. Dots and error bars represent medians from 250 corresponding model fits with shaded areas as 2.5%–97.5% percentiles. Blue dots represent outcome of 250 corresponding model fits (Section 2.6). Jitter on blue dots indicates uncertainty of adjusted rates by feed pump inaccuracy (2%). CDW, cell dry weight; IPTG, isopropyl- β -D-1-thiogalactopyranoside; STR, stirred tank bioreactor [Color figure can be viewed at wileyonlinelibrary.com]

laboratory scale STRs with minimized hands-on time. Moreover, high quality at-line data could be acquired at feasible temporal resolution and kinetic modeling was successfully applied to extract relevant KPIs.

3.3 | Application study I: Automated induction

The metabolic burden introduced by heterologous protein expression often comes along with a negative influence on quantity-related (e.g., titer, space-time-yield) and quality-related (e.g., product stability, by-products) aspects of a target process (Marschall et al., 2016). To optimize performance, inducible systems are widely used allowing initial biomass formation without detrimental effects. Accordingly, induction is a critical design aspect and requires special attention. Optimal production can be achieved if inducer dosage is triggered when exceeding a certain threshold in biomass concentration that has been determined in advance. The identification of optimal induction profiles requires several experiments (Kilikian et al., 2000). At laboratory scale, this is typically achieved by manual operation where the operator checks the condition of the culture at suitable intervals and decides on the time of inducer addition based on the data obtained.

In this application study, such task was automated by extending the workflow from Section 3.2: After each measuring cycle, the actual biomass concentration was compared with a predefined threshold and, if it was once exceeded, a defined amount of IPTG was dosed into the corresponding STR. Four different induction thresholds were tested in four STRs running in parallel and model-based analysis (Supporting Information Section 1.2) of the relationship between biomass threshold for induction and corresponding product concentration were derived.

Induction was implemented as event step determining the sudden change in the model behavior by using two different $Y_{\text{P/X}}$, namely before and after induction. The modified model resulted in a good match between predictions and experimental data (Figure 55). A functional relationship between final GFP titer and biomass threshold for induction could be derived (Figure 5a) which essentially predicts high product titer for induction at low biomass concentrations. Since the employed strain shows significant heterologous GFP secretion without IPTG addition, the observed range is rather narrow (~ 1.3 – 1.8 g L^{-1}). This observation is supported by a low change in q_{Pmax} upon IPTG addition (40% increase, Table 2). Thus, the predictions revealed a low sensitivity of this strain for GFP secretion with respect to inducer addition which agrees with previous experiments (unpublished data). In contrary, the model predictions confirmed the

TABLE 2 Fitting results and derived KPIs of the application study “automated induction”

	μ_{\max} (h ⁻¹)	basal $q_{P\max}$ (g·g ⁻¹ ·h ⁻¹)	induced $q_{P\max}$ (g·g ⁻¹ ·h ⁻¹)
Median	0.43	0.055	0.077
2.5%–97.5% percentile	0.38–0.47	0.038–0.067	0.067–0.094

Note: Median values and uncertainties derived from 250 model fits per cultivation set (Section 2.6).

growth rate (Table 2) from the previous proof-of-concept study (Section 3.2).

However, the demonstrated potential of this approach is apparent: to enable model-based design of bioprocesses to optimize typical KPIs (here, titer), bioprocess models with sufficient predictive power are required. The parallelized and automated data acquisition from STRs, the by far most relevant bioreactor configuration, lays the foundation for gaining the required information-rich experimental data.

3.4 | Application study II: Feed rate screening

Industrially relevant bioprocesses are often performed in fed-batch mode, where the limiting substrate is continuously fed. This offers extended process control and prevents detrimental effects of high substrate concentrations (Section 1). Among the most important process parameters of a fed-batch is the feed rate, which can have direct influence on KPIs (Hemmerich, Labib, et al., 2020).

In the presented application study, two different exponential feed rates were set per STR vessel, each being hold for a certain timespan. The workflow validated in Section 3.2 was used with few adaptations: Four STRs were set up with identical batch phases using 5 g L⁻¹ glucose as carbon source. After glucose consumption, feed pumps were started with the first set of feed rates. After 5 h, feed rates were changed to the second set, resulting in a total of eight different feed rates tested. During feed phases samples were drawn and processed every 30 min. The resulting data was used to fit the parameters of a fed-batch bioprocess model (Supporting Information Section 1.3).

GFP concentration in all four STRs rose over time depending on the applied feed rate, as exemplified in Figure 4b. As expected, higher feed rates (0.15–0.3 h⁻¹) showed comparably low $Y_{P/X}$, ranging from 0.13 to 0.20 g g⁻¹, while the lower feed rates (0.1 and 0.075 h⁻¹) resulted in higher yields of 0.27 ± 0.06 and 0.30 ± 0.06 g g⁻¹, respectively as presented in Figure 5c. Such inverse $Y_{P/X} = f(\mu)$ relation has been described for the same strain with alternative secreted protein products in fed-batch (Hemmerich, Moch, et al., 2018). Further studies reported on similar observations during heterologous production of intracellular proteins in diverse host systems applying batch experiments without externally controlled growth rate. In particular, Heyland et al. (2011) explained their

observations by a redirection of metabolic flux to meet the increased energy demand from heterologous protein production, meaning that less protein synthesis capacity was available for biomass formation (e.g., ribosomal proteins). Bienick et al. (2014), Borkowski et al. (2016) and Klumpp et al. (2009) argued with modeling of growth rate-dependent ribosomal capacity, since these studies predict a competition between translational capacity for building, for example, ribosomal proteins and translation of recombinant mRNA whose synthesis is not controllable by the cell.

The straightforward adaptation from batch to fed-batch processing with only marginal adaptations of the experiment logics orchestrated by the PCS underlines the clear advantages of such modular platform approaches: different experimental designs can be implemented in rather short time facilitating time-efficient experimentation.

4 | CONCLUDING REMARKS

The presented study illustrates the development of an automated system for taking, processing, and analyzing samples gathered from widespread and flexible laboratory scale STR systems. A custom-made automation module was utilized for sterile coupling of the STRs with a liquid handling system. An open and customizable PCS implemented in Python orchestrated the execution of liquid handling and data analysis procedures. Data obtained by the automated workflows can be used to fit suitable bioprocess models, providing thorough estimates of KPIs, essential for assessing process economics and optimization.

Firstly, an appropriate sampling/dosing hardware was developed and manufactured to provide an interface between the robotic worktable and the STRs. This enabled at-line execution of sampling events to feed three validated optical assays, but also addition IPTG as an inducer of heterologous protein expression in the application studies. Due to the open nature of both the liquid handling hardware and the PCS, other assays that are specifically needed for further studies can be easily integrated.

The three application studies clearly demonstrated the benefits of the system: without a human operator present, samples were drawn at regular intervals and subsequently processed and analyzed. Depending on the experiment, induction was done automatically, triggered by a biomass measurement. The presented setup allows for complex experiments as shown for screening eight exponential feed rates in one experiment with only four STRs.

Since all analytical procedures were run at-line, results were available directly after the experiment to calibrate multistaged bioprocess models. This highlights the strength of combining the classical, flexible STR setup with an automated modular sampling and processing approach for bioprocess modelling, a task which benefits from high-quality cultivation data.

The developed workflow could be extended by integrating more sophisticated analytical devices, such as flow cytometry or mass spectrometry, to enable a more detailed characterization and

deeper understanding of the bioprocess of interest, but also deep-frozen sample storage is in reach for future applications. On the software side, not only the processing of the raw measurement data could be run at-line, but also their direct integration into bioprocess models for parameter estimation and fast model validation. This would allow for automatic, model-driven reconfiguration of running cultivation experiments to quickly target the most interesting process regions.

This presented combination of functionalities cannot be easily achieved by other bioprocess development tools as it combines the most prominent upsides of all utilized devices in a synergistic manner.

ACKNOWLEDGEMENTS

The *Corynebacterium glutamicum* strain used in this study was kindly provided by Prof. Dr. Roland Freud at the Institute of Bio- and Geosciences of Forschungszentrum Jülich GmbH. Funding was received from the Enabling Spaces Program “Helmholtz Innovation Labs” of the German Helmholtz Association to support the “Microbial Bioprocess Lab—A Helmholtz Innovation Lab”. Further funding was received by the German Federal Ministry of Education and Research (BMBF, projects: “Digitalization in Industrial Biotechnology,” grant no. 031B0463 and “BioökonomieREVIER_INNO: Entwicklung der Modellregion BioökonomieREVIER Rheinland”, grant no. 031B0918A). Open Access funding enabled and organized by Projekt DEAL.

CONFLICT OF INTERESTS

Holger Morschett and Niklas Tenhaef are involved in a patent application concerning aspects of the manuscript.

AUTHOR CONTRIBUTIONS

Study design, experimental work, data evaluation, manuscript writing: Holger Morschett and Niklas Tenhaef. *Study design, data evaluation, manuscript writing:* Johannes Hemmerich. *Experimental work:* Laura Herbst, Markus Spiertz, and Deniz Dogan. *Scientific supervision, manuscript revision:* Wolfgang Wiechert. *Scientific supervision, manuscript revision, funding acquisition:* Stephan Noack and Marco Oldiges.

DATA AVAILABILITY STATEMENT

The data that support the findings of this study are available from the corresponding author upon reasonable request.

ORCID

Stephan Noack  <http://orcid.org/0000-0001-9784-3626>

Marco Oldiges  <http://orcid.org/0000-0003-0704-5597>

REFERENCES

- Baumann, P., Hahn, T., & Hubbuch, J. (2015). High-throughput micro-scale cultivations and chromatography modeling: Powerful tools for integrated process development. *Biotechnology and Bioengineering*, 112(10), 2123–2133. <https://doi.org/10.1002/bit.25630>
- Ben-Kiki, O., Evans, C., & döt Net, I. (2009). YAML ain't markup language (YAML™) version 1.2. <https://yaml.org/spec/1.2/spec.html>
- Bienick, M. S., Young, K. W., Klesmith, J. R., Detwiler, E. E., Tomek, K. J., & Whitehead, T. A. (2014). The Interrelationship between promoter strength, gene expression, and growth rate. *PLOS One*, 9(10), e109105. <https://doi.org/10.1371/journal.pone.0109105>
- Bisswanger, H. (2014). Enzyme assays. *Perspectives in Science*, 1(1), 41–55. <https://doi.org/10.1016/j.pisc.2014.02.005>
- Borkowski, O., Goelzer, A., Schaffer, M., Calabre, M., Mäder, U., Aymerich, S., Jules, M., & Fromion, V. (2016). Translation elicits a growth rate-dependent, genome-wide, differential protein production in *Bacillus subtilis*. *Molecular Systems Biology*, 12(5), 870. <https://doi.org/10.15252/msb.20156608>
- Chmiel, H. (2011). *Bioprosesstechnik*. Spektrum Akademischer Verlag.
- Cline, B., Reinartz, B., Lloyd, B., Anthoff, D., Akhiyarov, D., Roberts, T., Uriarte, V., Arvid, J. B., Bremner, C., Burnett, J., Catarino, A., Cronyn, I., Dittrich, M., Dupras, V., Dupré, X., Earl, A., Fernandez, D., Frayne, J., Freitag, S., ...Yang, W. (2019). pythonnet. <http://pythonnet.github.io/>
- Cruz Bournazou, M. N., Barz, T., Nickel, D. B., Lopez Cárdenas, D. C., Glauche, F., Knepper, A., & Neubauer, P. (2017). Online optimal experimental re-design in robotic parallel fed-batch cultivation facilities. *Biotechnology and Bioengineering*, 114(3), 610–619. <https://doi.org/10.1002/bit.26192>
- Doig, S. D., Baganz, F., & Lye, G. J. (2006). High-throughput screening and process optimisation. In C. Ratledge, & B. Kristiansen (Eds.), *Basic biotechnology* (3rd ed.) pp. 289–306. Cambridge University Press.
- Funke, M., Buchenauer, A., Schnakenberg, U., Mokwa, W., Diederichs, S., Mertens, A., Müller, C., Kensey, F., & Büchs, J. (2010). Microfluidic BioLector—Microfluidic bioprocess control in microtiter plates. *Biotechnology and Bioengineering*, 107(3), 497–505. <https://doi.org/10.1002/bit.22825>
- Grünberger, A., van Ooyen, J., Paczia, N., Rohe, P., Schiendzielorz, G., Eggeling, L., Wiechert, W., Kohlheyer, D., & Noack, S. (2013). Beyond growth rate 0.6: *Corynebacterium glutamicum* cultivated in highly diluted environments. *Biotechnology and Bioengineering*, 110(1), 220–228. <https://doi.org/10.1002/bit.24616>
- Harris, C. R., Millman, K. J., van der Walt, S. J., Gommers, R., Virtanen, P., Cournapeau, D., Wieser, E., Taylor, J., Berg, S., Smith, N. J., Kern, R., Picus, M., Hoyer, S., van Kerkwijk, M. H., Brett, M., Haldane, A., delRío, J. F., Wiebe, M., Peterson, P., ... Oliphant, T. E. (2020). Array programming with NumPy. *Nature*, 585(7825), 357–362. <https://doi.org/10.1038/s41586-020-2649-2>
- Hemmerich, J., Labib, M., Steffens, C., Reich, S. J., Weiske, M., Baumgart, M., Rückert, C., Ruwe, M., Siebert, D., Wendisch, V. F., Kalinowski, J., Wiechert, W., & Oldiges, M. (2020). Screening of a genome-reduced *Corynebacterium glutamicum* strain library for improved heterologous cutinase secretion. *Microbial Biotechnology*, 13, 2020–2031. <https://doi.org/10.1111/1751-7915.13660>
- Hemmerich, J., Moch, M., Jurischka, S., Wiechert, W., Freudl, R., & Oldiges, M. (2018). Combinatorial impact of Sec signal peptides from *Bacillus subtilis* and bioprocess conditions on heterologous cutinase secretion by *Corynebacterium glutamicum*. *Biotechnology and Bioengineering*, 116, 644–655. <https://doi.org/10.1002/bit.26873>
- Hemmerich, J., Noack, S., Wiechert, W., & Oldiges, M. (2018). Microbioreactor systems for accelerated bioprocess development. *Biotechnology Journal*, 13, 1700141. <https://doi.org/10.1002/biot.201700141>
- Hemmerich, J., Tenhaef, N., Steffens, C., Kappelmann, J., Weiske, M., Reich, S. J., Wiechert, W., Oldiges, M., & Noack, S. (2018). Less sacrifice, more insight: Repeated low-volume sampling of microbioreactor cultivations enables accelerated deep phenotyping of microbial strain libraries. *Biotechnology Journal*, 14, 1800428. <https://doi.org/10.1002/biot.201800428>
- Hemmerich, J., Tenhaef, N., Wiechert, W., & Noack, S. (2021). pyFOOMB: Python framework for object oriented modelling of bioprocesses. *Engineering in Life Sciences*, 21(3–4), 242–257. <https://doi.org/10.1002/elsc.202000088>

- Heux, S., Poinot, J., Massou, S., Sokol, S., & Portais, J.-C. (2014). A novel platform for automated high-throughput fluxome profiling of metabolic variants. *Metabolic Engineering*, 25, 8–19. <https://doi.org/10.1016/j.ymben.2014.06.001>
- Heyland, J., Blank, L. M., & Schmid, A. (2011). Quantification of metabolic limitations during recombinant protein production in *Escherichia coli*. *Journal of Biotechnology*, 155(2), 178–184. <https://doi.org/10.1016/j.jbiotec.2011.06.016>
- Huber, R., Ritter, D., Hering, T., Hillmer, A.-K., Kensy, F., Müller, C., Wang, L., & Büchs, J. (2009). Robo-Lector—A novel platform for automated high-throughput cultivations in microtiter plates with high information content. *Microbial Cell Factories*, 8, 42. <https://doi.org/10.1186/1475-2859-8-42>
- Keilhauer, C., Eggeling, L., & Sahm, H. (1993). Isoleucine synthesis in *Corynebacterium glutamicum*: molecular analysis of the ilvB-ilvN-ilvC operon. *Journal of Bacteriology*, 175(17), 5595–5603. <https://doi.org/10.1128/jb.175.17.5595-5603.1993>
- Kilikian, B. V., Suárez, I. D., Liria, C. W., & Gombert, A. K. (2000). Process strategies to improve heterologous protein production in *Escherichia coli* under lactose or IPTG induction. *Process Biochemistry*, 35(9), 1019–1025. [https://doi.org/10.1016/S0032-9592\(00\)00137-0](https://doi.org/10.1016/S0032-9592(00)00137-0)
- Klumpp, S., Zhang, Z., & Hwa, T. (2009). Growth rate-dependent global effects on gene expression in bacteria. *Cell*, 139(7), 1366–1375. <https://doi.org/10.1016/j.cell.2009.12.001>
- Kreyenschulte, D., Paciok, E., Regestein, L., Blumich, B., & Büchs, J. (2015). Online monitoring of fermentation processes via non-invasive low-field NMR. *Biotechnology and Bioengineering*, 112(9), 1810–1821. <https://doi.org/10.1002/bit.25599>
- Lee, H. L. T., Boccazzi, P., Gorret, N., Ram, R. J., & Sinskey, A. J. (2004). In situ bioprocess monitoring of *Escherichia coli* bioreactions using Raman spectroscopy. *Vibrational Spectroscopy*, 35(1), 131–137. <https://doi.org/10.1016/j.vibspec.2003.12.015>
- Marques, M. P. C., Cabral, J. M. S., & Fernandes, P. (2010). Bioprocess scale-up: quest for the parameters to be used as criterion to move from microreactors to lab-scale. *Journal of Chemical Technology and Biotechnology*, 85(9), 1184–1198. <https://doi.org/10.1002/jctb.2387>
- Marschall, L., Sagmeister, P., & Herwig, C. (2016). Tunable recombinant protein expression in *E. coli*: enabler for continuous processing? *Applied Microbiology and Biotechnology*, 100(13), 5719–5728. <https://doi.org/10.1007/s00253-016-7550-4>
- McKinney, W. (2010). *Data structures for statistical computing in Python*. Austin, TX: Paper presented at the Proceedings of the 9th Python in Science Conference.
- Meissner, D., Vollstedt, A., van Dijk, J. M., & Freudl, R. (2007). Comparative analysis of twin-arginine (Tat)-dependent protein secretion of a heterologous model protein (GFP) in three different Gram-positive bacteria. *Applied Microbiology and Biotechnology*, 76(3), 633–642. <https://doi.org/10.1007/s00253-007-0934-8>
- Paczia, N., Nilgen, A., Lehmann, T., Gätgens, J., Wiechert, W., & Noack, S. (2012). Extensive exometabolome analysis reveals extended overflow metabolism in various microorganisms. *Microbial Cell Factories*, 11, 122. <https://doi.org/10.1186/1475-2859-11-122>
- Passonneau, J. V., & Lowry, O. H. (1993). *Enzymatic analysis: A practical guide*. Humana Press
- Peuker, T., Riedel, M., Kaiser, C., Ellert, A., Lenz, K., Elsholz, O., & Luttmann, R. (2004). At-line determination of glucose, ammonia, and acetate in high cell density cultivations of *Escherichia coli*. *Engineering in Life Sciences*, 4(2), 138–143. <https://doi.org/10.1002/elsc.200401910>
- Puskeiler, R., Kaufmann, K., & Weuster-Botz, D. (2005). Development, parallelization, and automation of a gas-inducing milliliter-scale bioreactor for high-throughput bioprocess design (HTBD). *Biotechnology and Bioengineering*, 89(5), 512–523. <https://doi.org/10.1002/bit.20352>
- Rohe, P., Venkanna, D., Kleine, B., Freudl, R., & Oldiges, M. (2012). An automated workflow for enhancing microbial bioprocess optimization on a novel microbioreactor platform. *Microbial Cell Factories*, 11, 144. <https://doi.org/10.1186/1475-2859-11-144>
- Sonnleitner, B., Locher, G., & Fiechter, A. (1992). Biomass determination. *Journal of Biotechnology*, 25(1), 5–22. [https://doi.org/10.1016/0168-1656\(92\)90107-K](https://doi.org/10.1016/0168-1656(92)90107-K)
- Tamburini, E., Marchetti, M. G., & Pedrini, P. (2014). Monitoring key parameters in bioprocesses using near-infrared technology. *Sensors*, 14(10), 18941–18959. <https://doi.org/10.3390/s141018941>
- Tohmola, N., Ahtinen, J., Pitkänen, J.-P., Parviainen, V., Joenväärä, S., Hautamäki, M., Lindroos, P., Mäkinen, J., & Renkonen, R. (2011). On-line high performance liquid chromatography measurements of extracellular metabolites in an aerobic batch yeast (*Saccharomyces cerevisiae*) culture. *Biotechnology and Bioengineering*, 16(2), 264–272. <https://doi.org/10.1007/s12257-010-0147-3>
- Unthan, S., Grünberger, A., van Ooyen, J., Gätgens, J., Heinrich, J., Paczia, N., Wiechert, W., Kohlheyer, D., & Noack, S. (2014). Beyond growth rate 0.6: What drives *Corynebacterium glutamicum* to higher growth rates in defined medium. *Biotechnology and Bioengineering*, 111(2), 359–371. <https://doi.org/10.1002/bit.25103>
- Virtanen, P., Gommers, R., Oliphant, T. E., Haberland, M., Reddy, T., Cournapeau, D., Burovski, E., Peterson, P., Weckesser, W., Bright, J., van der Walt, S. J., Brett, M., Wilson, J., Millman, K. J., Mayorov, N., Nelson, A. R. J., Jones, E., Kern, R., Larson, E., ... SciPy, C. (2020). SciPy 1.0: Fundamental algorithms for scientific computing in Python. *Nature Methods*, 17(3), 261–272. <https://doi.org/10.1038/s41592-019-0686-2>
- Vojinović, V., Cabral, J. M. S., & Fonseca, L. P. (2006). Real-time bioprocess monitoring: Part I: In situ sensors. *Sensors and Actuators B: Chemical*, 114(2), 1083–1091. <https://doi.org/10.1016/j.snb.2005.07.059>
- van der Walt, S., Colbert, S. C., & Varoquaux, G. (2011). The NumPy array: A structure for efficient numerical computation. *Computing in Science & Engineering*, 13(2), 22–30. <https://doi.org/10.1109/MCSE.2011.37>

SUPPORTING INFORMATION

Additional Supporting Information may be found online in the supporting information tab for this article.

How to cite this article: Morschett, H., Tenhaef, N., Hemmerich, J., Herbst, L., Spiertz, M., Dogan, D., Wiechert, W., Noack, S., & Oldiges, M. (2021). Robotic integration enables autonomous operation of laboratory scale stirred tank bioreactors with model-driven process analysis. *Biotechnology Bioengineering*. 118, 2759–2769. <https://doi.org/10.1002/bit.27795>